



Permeability of active layer sediments and groundwater runoff in Brattegg River catchment, SW Spitsbergen

Mirosław WAŚNIK* , Henryk MARSZAŁEK 
and Michał RYSIUKIEWICZ 

*Institute of Geological Sciences, Department of Applied Hydrogeology,
Wrocław University, Plac M. Borna 9, 50-204 Wrocław, Poland*

** corresponding author <miroslaw.wasik@uwr.edu.pl>*

Abstract: This paper presents the permeability of the permafrost active layer determined in the Brattegg River catchment (SW Spitsbergen) for the 6-years interval of 2005–2010. The field permeability measurements technique of weathered rocks on various geomorphological forms allows to assess the value of their hydraulic conductivity (k). High variability of k values, ranging from $6.37 \cdot 10^{-9}$ to $4.0 \cdot 10^{-3} \text{ m s}^{-1}$, indicates the permeability of rocks from very low in clay to very high in gravel-rock rubble. Among the geomorphological forms, the best permeability was observed in boulder covers and rock debris, and the lowest one in patterned ground. The obtained results were used to determine the groundwater runoff (q_{tot}), assuming the unit thickness of the active layer aquifer. The q_{tot} value from the Brattegg River catchment was calculated at 130 L s^{-1} , which is from 15% to 47% of the average surface runoff.

Keywords: Arctic, Svalbard, active layer aquifer, geomorphological forms.



Introduction

Multidisciplinary studies, identifying the processes responsible for progressive climate change, have been carried out for many years in the Bratteg River catchment (Migała *et al.* 2008; Owczarek 2010; Migoń and Kasprzak 2013; Marszałek and Górniak 2017). Increase in air temperature caused the glacier recession, development of young geomorphological forms and vegetation succession (Owczarek *et al.* 2014). Water from precipitation, melting glaciers, perennial permafrost and snow cover flows directly or indirectly into the sea in the form of surface and groundwater runoff in the Bratteg River catchment (Marszałek *et al.* 2013a). There is no evidence of a deep regional groundwater circulation beneath permafrost in this catchment, therefore groundwater runoff seems to form only during the Arctic summer within the subsurface active layer of permafrost. The volume of runoff strictly depends on its thickness and the permeability of the rocks that build it.

Studies of permeability of the active layer sediments and groundwater runoff have not been carried out to a greater extent in the polar regions. The hydrological studies conducted in the Arctic mostly focused on assessing of total or surface runoff (Pulina *et al.* 1984; Sobota 2000; Sobota *et al.* 2010; Bartoszewski and Michalczyk 2013; Marszałek *et al.* 2013a; Majchrowska *et al.* 2015). Groundwater presence in cold areas (Haldorsen and Heim 1999; Lemieux *et al.* 2016), the residence time of groundwater in the rock environment (Hiyama *et al.* 2013), the exchange of ground- and surface water (Ge *et al.* 2011) and changes in the groundwater runoff depending on the thawing of permafrost (St. Jacques and Sauchyn 2009; Walvoord *et al.* 2012; Duan *et al.* 2017; Evans *et al.* 2018; Lamontagne-Hallé *et al.* 2018) were also discussed. The influence of frequent freezing and thawing of sediments on their permeability and structure is relatively well recognized (Burt and Williams 1976; Chamberlain and Gow 1979; McKenzie *et al.* 2007; Watanabe and Flury 2008), as well as the relationships between hydraulic conductivity of the sediments and their saturation with water (Scheidegger 2013). In these works, the values of the hydraulic conductivity were not determined, but were taken from the literature, and the relationships were determined on the basis of calculations or modeling.

The attempts to separate the underground component of water flow from the active layer of permafrost are made rarely, mainly due to the lack of recognition of filtration parameters in unconsolidated rocks (Marciniak *et al.* 2011; Marszałek *et al.* 2013b; Lamontagne-Hallé *et al.* 2018). Difficulties in assessing groundwater runoff, which is often ignored (Hagen and Lafauconnier 1995; Killinqueit *et al.* 2003), affect the credibility of water balance calculations. Field studies of rock permeability, necessary for the accurate determination of groundwater runoff, are carried out rarely (Quinton *et al.* 2008; Kim *et al.* 2020; Chen *et al.* 2021). In Spitsbergen, this type of studies were completed only in the

Ebba River catchment located in the Petunia Bay area, but mainly well-permeable sediments were investigated (Marciniak *et al.* 2011).

The measurements of permeability of subsurface unconsolidated rocks, which have been conducted for the first time in the Brattegg River catchment, provided the information for the correct assessment of dynamic water flow in the top layers of permafrost. Permeability of active layer, expressed by hydraulic conductivity, influences groundwater flow and the velocity of pollutants migration. The Brattegg River catchment is a good test site because of its small area, recharged by the glacier located in its upper part, and the variety of sediments and geomorphological forms.

The main aim of this research was to assess the permeability of different sediments that build the active layer of permafrost in the Brattegg River catchment and in different surface geomorphological forms. Spatial differentiation of the hydraulic conductivity, that was evaluated from field investigations, enable to calculate the groundwater runoff for the aquifer. The volume of the groundwater runoff was compared with the total runoff determined from the measurements of the Brattegg River flow rate. The results, covering all major lithological types and geomorphological forms, can be used for more detailed analyses of the groundwater circulation within the active layer in other polar regions.

Study area

The Brattegg River catchment is located in Wedel Jarlsberg Land in the Sør-Spitsbergen National Park (SW Svalbard). With a surface area of 8.2 km², it belongs to a partly glaciated river-lake system composed of three lakes linked by the Brattegg River (Figs. 1 and 2). The Myrktjørn Lake, with the depth of 6.9 m, has the largest area of 1.4 km² (Marszałek and Górnjak 2017). The Brattegg River drains coastal parts of the western Spitsbergen during summer Arctic seasons, starting from small glacier and flowing towards the Greenland Sea. The hill-slope of the river valley in the upper part (6% on average) decreases below the Myrktjørn Lake outflow, where it reaches a flat sea terrace level. Two main types of relief were distinguished in the catchment: (i) mountainous terrain with widespread debris and valleys partially covered with glaciers, rock glaciers and (ii) coastal platform with a system of raised marine terraces, occurring in the studied catchment up to an altitude of 80 m a.s.l. (Migoń and Kasprzak 2013) (Fig. 1). The coastal zone is dominated by a strandflat, *i.e.*, a wide platform at an elevation of 4–25 m a.s.l. with well-rounded marine pebbles. On the ground surface, various periglacial forms such as patterned ground, solifluction stripes and lobes, orthogonal frost crack networks and spotted tundra surfaces with “islands” of clayey material, surrounded by larger clasts and debris, are observed. Mountain slopes are mainly covered by rock, talus or debris-mantled slope with boulders and finer debris (Migoń and Kasprzak 2013).

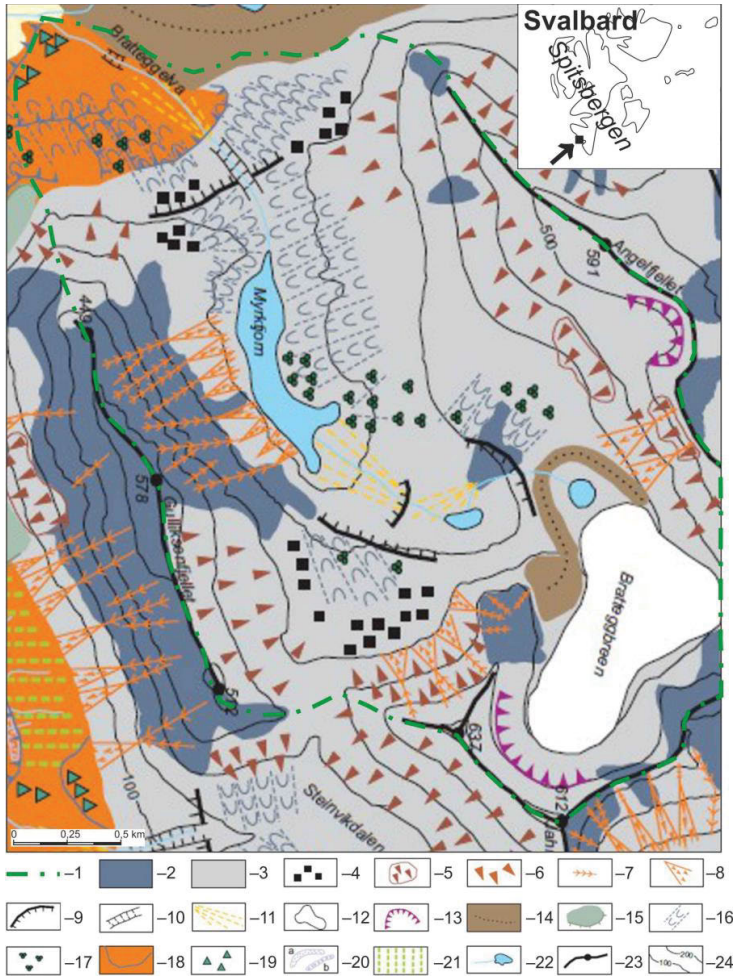


Fig. 1. Geomorphological map of the Brattegg catchment after Migoń and Kasprzak (2013): 1 – catchment boundary, 2 – rock slopes, 3 – debris mantled slopes, 4 – talus, 5 – boulder blankets, compact, 6 – boulder blankets, dispersed, 7 – ravines and chutes, 8 – scree cones, 9 – rock steps, 10 – erosional incisions, 11 – alluvial fans, 12 – glaciers, 13 – edges of glacial cirques, 14 – moraine ridges, 15 – rock glaciers, 16 – solifluction stripes and lobes, 17 – patterned ground, 18 – raised marine terraces, 19 – sea stacks, 20 – storm ridges, 21 – organogenic cover deposits, 22 – streams and lakes, 23 – selected ridges and peaks, 24 – contour lines.

The climatic conditions are characterized by low average annual temperatures (-2.1°C) and limited precipitations of 422 mm on average, with variations from 230 mm in the dry year (1987) to 635 mm in the wet one (1996). Permanent snow cover usually occurs in the second half of September and lasts generally until the first decade of June (Kwaczyński 2003; Przybylak and Arażny 2006). Snow is the dominant form of precipitation during the year (Marsz *et al.* 2013).

The daily Brattegg river discharge usually changes during the summer season, from late June to mid-July exceeding $1\text{ m}^3\text{ s}^{-1}$ (sometimes $>1.5\text{ m}^3\text{ s}^{-1}$),

and from late July to August it decreases markedly to $<0.5 \text{ m}^3 \text{ s}^{-1}$. Some peak flows $>2 \text{ m}^3 \text{ s}^{-1}$ were observed (Stachnik *et al.* unpublished).

Geologically, the Brattegg River catchment is composed of Middle Proterozoic metamorphic rocks of several crystalline formations including mainly amphibolites, mica-schists, quartzites of the Brattegg Valley Formation and white or green quartzites of the Gullichsenfjellet Formation (Czerny *et al.* 1993; Birkenmajer 2013) (Fig. 2). Crystalline rocks are covered by sands and sea gravels, forming terraces and boulder fields in the coastal zone. Inside the catchment area, excluding the highest mountain parts, the weathered cover with the admixture of various clay fractions, can be found. The river valleys are filled with coarse clastic material. In the upper part of the catchment, moraines are common. They formed as a result of local glacier advances or stillstands.

Groundwater outflows, occurring in the studied catchment during the summer season, represent the shallowest circulation system associated with the subsurface zone of the bedrock lying above the permafrost. Their presence is related to the drainage of the active layer of permafrost, formed in the well-permeable upper parts of weathered crystalline rocks. There is no evidence of deeper groundwater circulation, *i.e.*, subpermafrost aquifer, in the catchment (Modelska and Buczyński 2023).

Materials and methods

The permeability of the subsurface profile of the active layer was directly determined by field measurements during the summer seasons (July–August) of 2005–2010. The tested sediments were completely defrosted during the investigations. These measurements were preceded by detailed geological mapping aimed to assess the variability of lithology across the selected transects running through the Brattegg River catchment (Fig. 2).

In order to determine the permeability of the unconsolidated rocks, field study was carried out to assess the hydraulic conductivity (k), using two methods: the Porschet method (23 measurements) and the double-ring infiltrometer (Giryński's method, after Pazdro and Kozerski 1990) (41 measurements). Their locations are shown on Fig. 2. The measurements using the Porschet method were conducted in those locations where it was not possible to press the double-ring infiltrometer, into the ground. Both methods are complementary, providing similar results (Wąsik 2003).

Using the Porschet method, the velocity of infiltrating water was measured three times in a drilled hole with a depth of ~ 50 cm and a diameter of ~ 12 cm. The drilled hole was filled with water and the height of the water table above the bottom was measured at specified intervals (Fig. 3a). The following formulas were used for the calculations of k (Pleczyński 1981):

$$k = \frac{[\varphi(x_1) - \varphi(x_2)]}{\Delta t} \quad (1)$$

where:

$$\varphi(x_1) = \frac{r}{2}(\log x_1 + \frac{r}{2}),$$

$$\varphi(x_2) = \frac{r}{2}(\log x_2 + \frac{r}{2}),$$

$$\Delta t = t_2 - t_1,$$

k - hydraulic conductivity (m s^{-1}),

x_1, x_2 - the height of the water table above the bottom of the hole (m),

t_1, t_2 - time of lowering the water table from x_1 to x_2 (s),

r - the drilled hole diameter (m).

In order to measure the permeability using the Eijkelkamp double-ring field infiltrometer, two rings (Fig. 3b) were hammered concentrically to a depth of

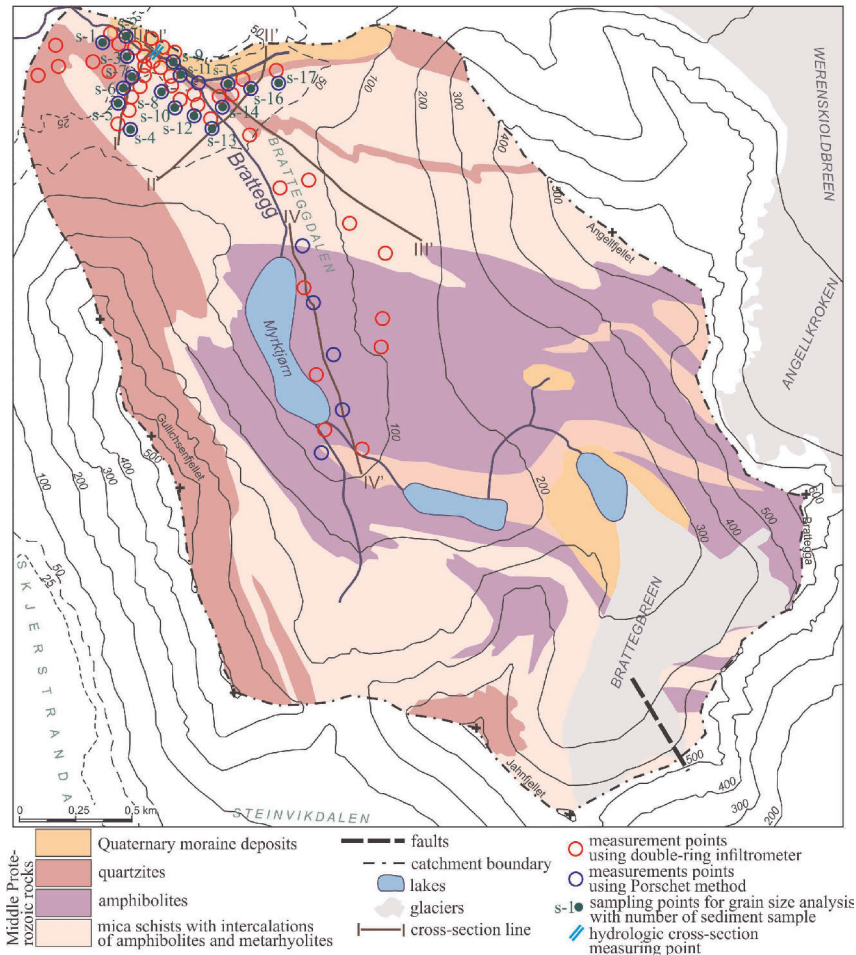


Fig. 2. Geological map of the Brattegg catchment after Czerny *et al.* (1993) with location of permeability measurements points and sampling.



Fig. 3. Field measurement of sediment permeability using Porschet method (A) and the Eijkelkamp double-ring infiltrometer (B).

several centimeters of the sediment. Then, water was poured into both rings and decrease of the water level was measured. Water infiltrated from the outer ring saturates the sediment below the infiltrometer and formed a buffer zone. This caused holding the water inside of the inner ring where the infiltration measurement was conducted. Measurements have been repeated three times to mirror the prevailing conditions in the saturated and the unsaturated zone at the measurement site. It was assumed that the rate of infiltration is approximately equal to the permeability of the unsaturated zone (Eijkelkamp 1983). The infiltration rate was determined by measuring the drop in the height of the water column in the infiltrometer per unit time.

The hydraulic conductivity k is related to the grain-size distribution of granular porous media (Freeze and Cherry 1979), therefore, a grain-size analysis was conducted for 17 sediment samples. They were collected only in the lower part of the catchment area in 2009, mainly due to better development of investigated geomorphological forms and easier access. The grain size analyses enabled to identify the sand, gravel and pebbles, while pipette analysis discriminated between silt and clay fractions. Fractions coarser than pebbles were not taken into account. Both analyses were conducted following published guidelines (Myślińska 2001) in the Laboratory of Soil Mechanics Institute of Geography and Regional Development, Wrocław University.

The main grain indexes were calculated using the formulas after Racinowski *et al.* (2001) in order to characterize the investigated sediments based on diameters expressed in phi units:

M_z – average grain size

$$M_z = \frac{\Phi_{16} + \Phi_{50} + \Phi_{84}}{3} \quad (2)$$

δ_I – standard deviation (graphical standard deviation), or sorting

$$\delta_I = \frac{\Phi_{84} - \Phi_{16}}{4} + \frac{\Phi_{95} - \Phi_5}{6.6} \quad (3)$$

S_{kl} – skewness (graphic skewness)

$$S_{kl} = \frac{\Phi_{84} - \Phi_{50}}{\Phi_{84} - \Phi_{16}} - \frac{\Phi_{50} - \Phi_5}{\Phi_{95} - \Phi_5} \quad (4)$$

K_G – flattening of the grain size distribution

$$K_G = \frac{\Phi_{95} + \Phi_5}{2.44(\Phi_{75} - \Phi_{25})} \quad (5)$$

U – graining uniformity coefficient

$$U = \frac{d_{60}}{d_{10}} \quad (6)$$

where:

$\Phi_5, 16, 25, 50, 75, 84, 95$ – grain diameters, which together with smaller grains on the phi scale (larger in mm) account for 5%, 16%, 25%, 50%, 75%, 84%, 95% of the sediment sample weight, respectively,

d_{60} i d_{10} – grain diameters (in mm), which together with smaller grains account for 60% and 10%, respectively.

Using the sediment permeability data, the amount of the groundwater runoff (q) within the individual lithological types and geomorphological forms was calculated, for the accepted unit values of the aquifer thickness (m) and the groundwater stream width (B). The total groundwater runoff (q_{tot}) from the Bratęgg River catchment was also calculated, for the assumed m of 1 m. The calculations were based on the measurements carried out in the period of 2007–2009. For the calculations purposes the formula below was used (Freeze and Cherry 1979; Pazdro and Kozerski 1990):

$$q_{tot} = k \frac{\Delta H}{\Delta l} m B \quad (7)$$

where:

q_{tot} – the amount of groundwater flow ($L s^{-1}$),

k – hydraulic conductivity ($m s^{-1}$),

$\frac{\Delta H}{\Delta l}$ – hydraulic drop, pressure difference to the distance over which it occurs,

m – thickness of the water layer (m),

B – width of the groundwater stream (m).

The amount of the groundwater runoff in the summer season is primarily determined by the active layer thickness and the permeability of rocks expressed by the k values, which are variable. Rock permeability depends, among others, on the defrosting degree of the aquifer or water temperature. In the calculations of the groundwater runoff, the unit thickness of the aquifer and the constant k value

determined for completely thawed rocks were assumed. In order to calculate the groundwater runoff to the Brattegg River, the average values of the hydraulic conductivity of rocks and geomorphological forms lying on both sides of the river were determined. Due to lack of data on changes in the thickness of the melted active layer in the summer season, the authors did not have the opportunity to compare different states of groundwater runoff and river flows. The results were compared with the average river discharge, *i.e.*, surface runoff, measured in the hydrometric gauge cross-section installed in the lower part of the Brattegg River catchment at 24 m a.s.l. (Stachnik *et al.* unpublished). This enable to roughly assess which part of the total runoff constitute the groundwater runoff. The propeller-type current meter OTT C31, with measurement range from 0.025 to 10 m s⁻¹ and accuracy $\pm 2\%$, was used to measure the Brattegg River flow rate.

Results and interpretation

Characteristics of the active layer sediments. — Based on the field macroscopic observation and the results of grain size analyses of loose sedimentary rocks found in the Brattegg River catchment (Fig. 4), seven main lithological types were distinguished: loams, sandy loams, sand with debris, multi-grained sand, pebbly debris, sand-gravel debris and loamy debris. These materials were deposited in sedimentary environments characterized by different dynamics, indicated by significant variations in the calculated values of the average grain size (Tables 1 and 2). Moreover, very weak or extremely weak sorting of δ_I of all tested sediments indicates a variable dynamics of the environment during their deposition (Czyżewska 1997; Racinowski *et al.* 2001). Such sorting (δ_I values 2.49–4.64) is typical for sediments formed as a result of slope processes or direct accumulation of the glacial material, *e.g.*, boulders of bottom moraine. An uneven grain size distribution is also indicated by high values of the graining uniformity coefficient, usually *ca.* 10–500.

The skewness (S_{kl}) of the graining distributions of the studied sediments varies from very negatively oblique to very positive oblique, S_{kl} values ranging from -0.47 to 0.73. It also indicates a wide range of the sedimentation environment dynamics. Negative values indicate the enrichment of the material with coarser fractions, and positive values indicate the opposite process, *i.e.* bringing fine fractions to the sediment. Such a distribution of S_{kl} values indicates that the sedimentation was related not only to non-current environments (deluvial sediments, loam), which are usually characterized by positive skewness (Łanczont 1994), but also other environments, *e.g.*, aquatic and aeolian.

The characteristics of the K_G flattening of the grain size distribution indicate different environments of loose material deposition. Non-current sludge is characterized by low K_G values. 75% of the studied sediments have a platykurtic or very platykurtic particle size distribution ($K_G < 0.9$), which indicates variable

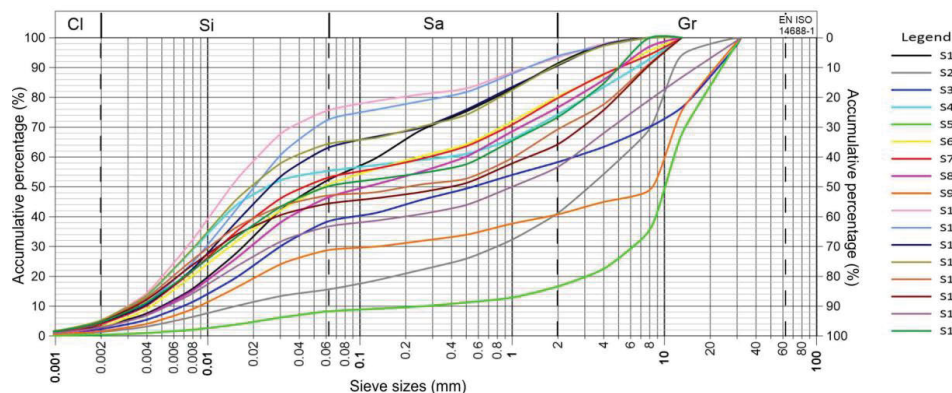


Fig. 4. Grain-size distribution curves of selected active layer types of loose rocks. The sample numbers in the legend are in accordance with Fig. 2.

conditions during their sedimentation, high saturation of the sedimentation environment with mineral material and an initial stage of sediment differentiation (Racynowski *et al.* 2001). In several sediment samples, the particle size distribution was mesokurtic ($K_G = 1.06$ in a sample of gravel and debris), leptokurtic ($K_G = 1.13$ and 1.29 in two clay samples with pebbly debris) and very leptokurtic ($K_G = 2.09$ in a sample of sandy-gravel debris and loamy debris). The leukokurtic nature of the particle size distribution indicates a selective deposition.

Characteristics of sediments permeability. — The permeability of the active layer sediments is primarily determined by the content of the fine fraction and the size of the pores, uniformity of the graining and the representative diameter of the grains. The obtained k values of sediments vary from $6.37 \cdot 10^{-9}$ to $4.0 \cdot 10^{-3} \text{ m s}^{-1}$ (Table 3). Such a range of values proves their different permeability. The lowest permeability, very low and low according to Dowgiałło *et al.* (2002), is mostly typical for clays (k ranging from $6.37 \cdot 10^{-9}$ to $8.99 \cdot 10^{-7} \text{ m s}^{-1}$). Sandy loams and loamy debris (k from $2.60 \cdot 10^{-7}$ to $7.57 \cdot 10^{-5} \text{ m s}^{-1}$) have slightly higher permeability, *i.e.*, from low to medium. Various types of debris and different-grained sands, with k values ranging from $6.09 \cdot 10^{-6}$ to $1.69 \cdot 10^{-3} \text{ m s}^{-1}$, are more permeable, *i.e.*, fall into medium to very high permeability class. The highest permeability, *i.e.*, high and very high and with k values from $1.75 \cdot 10^{-4}$ to $1.69 \cdot 10^{-3} \text{ m s}^{-1}$, is typical for gravel and pebbly debris.

Most of the studied formations can be described as non-insulating, only sandy loams and loamy debris have very poor insulation properties, and the loams are poorly and very poorly insulating (Table 3). The degree of insulation indicates the presence of relatively favorable conditions for groundwater supply in the Brattegg River catchment as a result of rainwater or surface water infiltration.

Permeability characteristics of geomorphological forms. — The characteristics of the geomorphological forms occurring in the Brattegg River catchment take into account the results of permeability tests of the sediments that formed them (Table 4). Pebble sediments and boulder covers are characterized by

Table 1.

Graining parameters of the clastic rocks in the Brattegg River catchment.

Indicator	Measurement location																
	s1	s2	s3	s4	s5	s6	s7	s8	s9	s10	s11	s12	s13	s14	s15	s16	s17
	values on the phi scale																
Average grain size M_Z	4.26	-1.67	0.88	5.29	-3.45	4.10	4.48	3.18	-3.04	6.13	5.61	5.26	5.68	2.27	1.42	0.01	4.04
Average diameter S_S	3.70	-0.46	1.00	3.68	-2.93	3.32	3.48	2.76	-0.45	4.94	4.62	4.24	4.44	2.52	2.18	1.05	3.21
Standard deviation (sort) δ_I	3.30	3.62	4.64	4.32	2.49	3.97	4.06	3.88	4.51	3.34	3.29	3.49	3.62	4.42	4.42	4.59	4.12
Skewness S_{kl}	-0.19	0.53	0.08	-0.45	0.58	-0.24	-0.31	-0.10	0.74	-0.47	-0.39	-0.36	-0.42	0.07	0.22	0.30	-0.21
Flattening K_G	0.80	1.06	0.57	0.61	2.09	0.68	0.68	0.67	0.58	1.30	1.13	0.76	0.69	0.58	0.58	0.63	0.61
Graining uniformity coefficient U	24	344	320	121	65	57	75	91	1294	7	8	12	11	303	364	436	171

Table 2.
 Characteristics of sediments graining in the Brattegg River catchment.

Sediment category	Sample number	Share of granulometric fractions					Average grain size M_Z	Average diameter S_S	Standard deviation (sort) δ_f	Skewness S_{kt}	Flattening K_G	Graining uniformity coefficient U
		clay	silt	sand	gravel	pebbles						
values in %												
Loam	s4, s13, s14, s15	1.40–1.69	32.68–44.29	22.07–36.51	17.51–42.13	0	1.42–5.68	2.17–4.44	3.62–4.42	–0.45–0.22	0.58–0.69	11–364
Sandy loam	s7, s8	0.95–1.28	25.33–33.92	35.68–42.31	19.12–31.42	0	3.18–4.48	2.76–3.48	3.88–4.06	–0.31––0.10	0.67–0.68	75–91
Loam with debris	s10, s11, s16, s17	1.02–1.55	22.43–51.09	26.58–45.16	11.55–36.72	0–13.24	0.01–6.12	1.05–4.94	3.29–4.57	–0.47–0.30	0.60–1.29	7–436
Multi-grained sand	s1	1.17	26.88	54.86	17.09	0	4.26	3.70	3.30	–0.19	0.80	24
Debris	s2, s9, s12	0.42–1.60	9.70–36.89	21.32–45.02	16.49–61.85	0–24.54	–3.04–5.26	–0.46–4.24	3.49–4.50	–0.36–0.73	0.58–1.06	12–1294
Loamy debris	s3, s5, s6	0.17–0.85	3.70–31.12	9.03–40.05	22.61–54.79	0–32.30	–3.45–4.10	–2.93–3.32	2.49–4.64	–0.24–0.58	0.57–2.09	57–320

Table 3.

Characteristics of sediments permeability in the Brattegg River catchment.

Sediment category	Number of measurements	Hydraulic conductivity k (m s^{-1})				Permeability class (Dowgiało <i>et al.</i> 2002)	Class of insulating rocks (Dowgiało <i>et al.</i> 2002)
		min.	max.	weighted average	standard deviation		
Loam	8	$6.37 \cdot 10^{-9}$	$8.99 \cdot 10^{-7}$	$3.22 \cdot 10^{-7}$	$3.08 \cdot 10^{-7}$	very low–low	poorly–very poorly insulating
Sandy loam	3	$2.60 \cdot 10^{-7}$	$5.24 \cdot 10^{-6}$	$2.91 \cdot 10^{-6}$	$2.51 \cdot 10^{-6}$	low–weak	very poorly insulating–non-insulating
Sand with debris	8	$7.04 \cdot 10^{-7}$	$7.57 \cdot 10^{-5}$	$1.76 \cdot 10^{-5}$	$2.52 \cdot 10^{-5}$	low–medium	very poorly insulating–non-insulating
Multi-grained sand	2	$1.45 \cdot 10^{-5}$	$2.22 \cdot 10^{-4}$	$1.18 \cdot 10^{-4}$	$1.47 \cdot 10^{-4}$	medium–high	non-insulating
Pebbly debris	12	$1.75 \cdot 10^{-4}$	$4.00 \cdot 10^{-3}$	$1.69 \cdot 10^{-3}$	$1.46 \cdot 10^{-3}$	high–very high	non-insulating
Sandy-gravel debris	14	$3.14 \cdot 10^{-5}$	$1.00 \cdot 10^{-3}$	$3.64 \cdot 10^{-4}$	$3.18 \cdot 10^{-4}$	medium–high	non-insulating
Loamy debris	17	$6.09 \cdot 10^{-6}$	$3.12 \cdot 10^{-4}$	$8.20 \cdot 10^{-5}$	$9.19 \cdot 10^{-5}$	weak–high	non-insulating

Table 4.

Characteristics of the geomorphological forms permeability in the Bratregg River catchment.

Geomorphological forms	Number of measurements	Hydraulic conductivity k ($m s^{-1}$)			Permeability class (Dowgiatto <i>et al.</i> 2002)	Class of insulating rocks (Dowgiatto <i>et al.</i> 2002)	Lithological types
		min.	max.	weighted average standard deviation			
Rocky initial soils	3	$2.15 \cdot 10^{-5}$	$1.75 \cdot 10^{-4}$	$3.68 \cdot 10^{-5}$ $8.55 \cdot 10^{-5}$	medium-high	non-insulating	debris, loamy debris
Sorted patterned ground (middle part)	12	$6.37 \cdot 10^{-9}$	$5.09 \cdot 10^{-6}$	$5.89 \cdot 10^{-8}$ $1.40 \cdot 10^{-6}$	very low-weak	poorly insulating-non-insulating	loam, sandy loam, loam with debris
Sorted patterned ground (outer part)	6	$5.24 \cdot 10^{-6}$	$7.69 \cdot 10^{-4}$	$1.28 \cdot 10^{-5}$ $3.16 \cdot 10^{-4}$	weak-high	non-insulating	debris, loamy debris, loam with debris, sandy loam
Pebbly alluvial sediments	13	$6.09 \cdot 10^{-6}$	$6.52 \cdot 10^{-4}$	$2.89 \cdot 10^{-5}$ $2.10 \cdot 10^{-4}$	weak-high	non-insulating	debris, loamy debris, multi-grained sand
Boulder blankets	4	$4.76 \cdot 10^{-4}$	$1.54 \cdot 10^{-3}$	$5.74 \cdot 10^{-4}$ $5.55 \cdot 10^{-4}$	high-very high	non-insulating	debris
Solifluction stripes	9	$6.68 \cdot 10^{-6}$	$7.14 \cdot 10^{-4}$	$3.72 \cdot 10^{-5}$ $2.20 \cdot 10^{-4}$	weak-high	non-insulating	debris, loamy debris, loam with debris
Talus	9	$1.43 \cdot 10^{-4}$	$4.00 \cdot 10^{-3}$	$7.35 \cdot 10^{-4}$ $1.55 \cdot 10^{-3}$	high-very high	non-insulating	debris
Nonsorted patterned ground	8	$3.24 \cdot 10^{-6}$	$1.13 \cdot 10^{-4}$	$1.52 \cdot 10^{-5}$ $3.76 \cdot 10^{-5}$	weak-high	non-insulating	loamy debris, loam with debris, sandy loam

the highest k , estimated at $7.35 \cdot 10^{-4} \text{ m s}^{-1}$ and $5.74 \cdot 10^{-4} \text{ m s}^{-1}$, respectively. These values determine the permeability of sediments filling the space between larger boulders, with an average diameter of several dozen centimeters, but also larger. The lowest permeability with the order of 10^{-9} to 10^{-6} m s^{-1} was determined for the central part of the sorted patterned ground built of clayey material. Much more permeable (k values $5.24 \cdot 10^{-6}$ to $7.69 \cdot 10^{-4} \text{ m s}^{-1}$) are the outer parts of the grounds due to the greater share of coarser particles. Similar permeability (mean k of the order of 10^{-5} to 10^{-4} m s^{-1}) is observed in the remaining geomorphological forms (Table 4).

In the Brattegg River catchment, a large variation in the permeability of sediments within a given geomorphological form is observed, due to the presence of several lithological types in each form. Moreover, at a relatively short distance, a high variability of geomorphological forms may be observed (Fig. 5).

In the studied catchment, the more permeable sediments can be found usually in the marginal and channel parts of the river valley. The edge parts of the valley, adjacent to mountain slopes or a lateral moraine, are often covered with rock sediments and boulder covers. The Brattegg River bed is filled with coarse-grained river sediments, e.g., pebbly alluvial sediments, whereas the bottom of the valley is filled with sediments of different, generally weaker permeability. This creates a system where supply and drainage zones contain sediments with higher permeability, and in the transit zone of groundwater flow sediments show lower permeability. Such conditions in the marginal part of the Brattegg valley facilitate the recharge of groundwater during the summer season in the melted layer of permafrost, as a result of rainwater infiltration and lateral inflow of waters flowing from the mountain slopes surrounding the valley. On the contrary, the lower permeability of the sediments at the bottom of the valley impedes the outflow of groundwater to the drainage zone, which is the Brattegg river bed. In regions with lower sediments permeability, groundwater flowing from the edge of the valley and from melted permafrost are dammed up, as a result of which the water table is closer to the ground surface. Therefore, in these regions, the waterlogged grounds can be often observed.

Groundwater runoff in active layer. — The value of the groundwater runoff is determined by the three parameters: rock permeability determined by the values of the hydraulic conductivity, the thickness of the aquifer and the hydraulic gradient. The most important in that case is the permeability due to its possible high variability, even within the same lithological type. Our calculations seem reliable owing to the use of field results.

In order to explore ways of forming the groundwater runoff within individual lithologies and geomorphological forms, the values of the unit groundwater runoff q were calculated. Unit values were adopted for the thickness of the aquifer ($m = 1 \text{ m}$) and the width of the groundwater stream ($B = 1 \text{ m}$). Due to the shallow water table from a few cm to $>1 \text{ m}$ below the ground level and the lack of precise knowledge on its depth, the value of the hydraulic gradient of 0.05 was

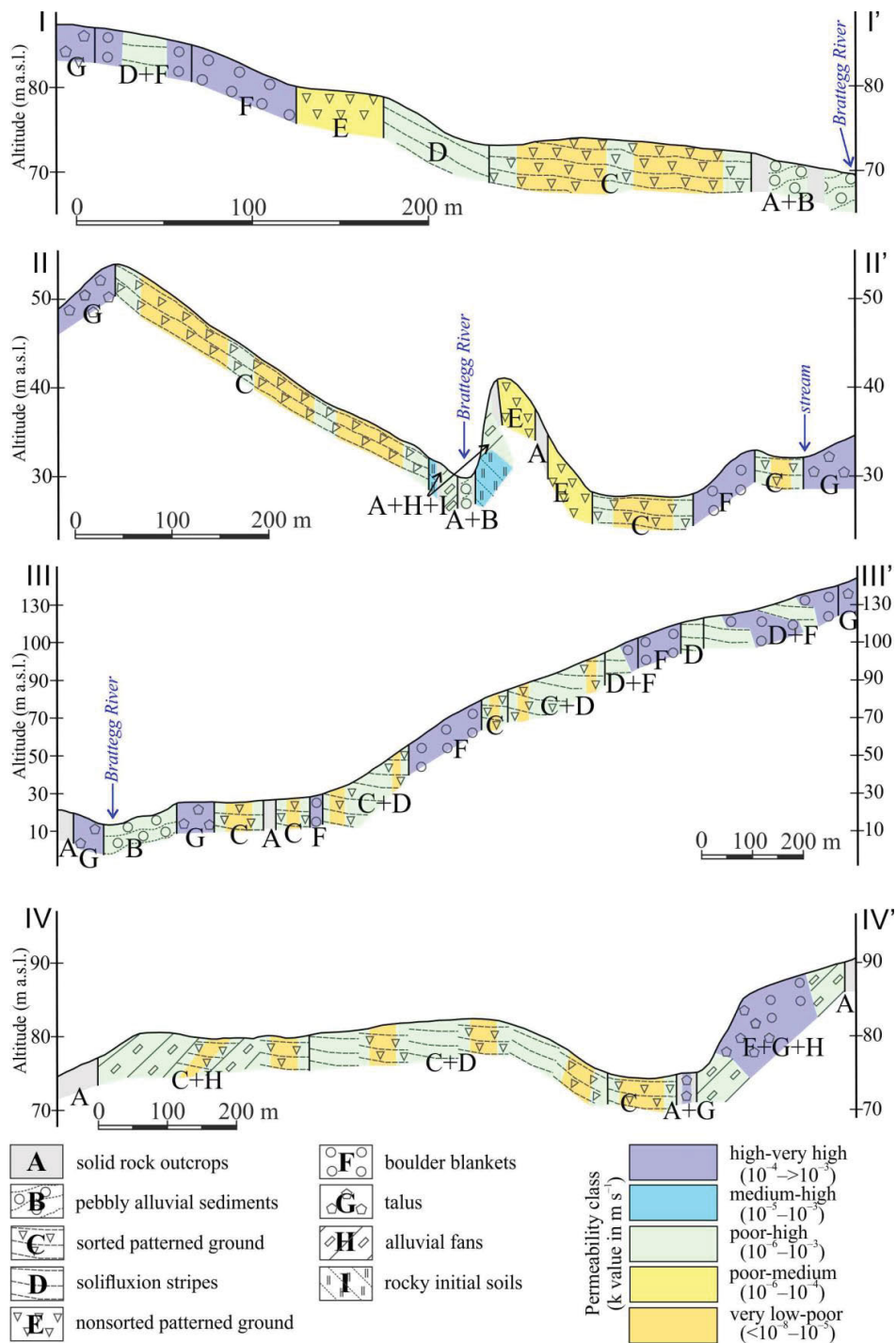


Fig. 5. Geological cross-sections through the Brattegg River catchment. The cross-section lines comply with Fig. 2.

assumed for the calculations, corresponding to the slope of the bottom part of the Brattegg River valley.

The obtained results indicate extremely different conditions of groundwater flow formation inside of the studied sediments (Table 5). The flow with the highest intensity in the range from $8.75 \cdot 10^{-3}$ to 0.20 L s^{-1} ($8.45 \cdot 10^{-2} \text{ L s}^{-1}$ on average) may occur in the area of gravel and rock debris, and the lowest one in loams, ranging from of $3.18 \cdot 10^{-7}$ to $4.49 \cdot 10^{-5} \text{ L s}^{-1}$ ($1.61 \cdot 10^{-5} \text{ L s}^{-1}$ on average).

For geomorphological forms, the most favorable conditions for the flow of groundwater occur when land is covered by rock debris, pebbly and boulder sediments. The average values of q calculated for these geomorphological forms are $3.67 \cdot 10^{-2}$ and $2.87 \cdot 10^{-2} \text{ L s}^{-1}$, respectively (Table 5). On the other hand, the worst conditions for shaping the groundwater flow occur in the areas where sorted patterned ground has been developed. Within their central, more clayey part, the flow of groundwater is practically impossible, with the mean value of the unit flow q reaching only $2.94 \cdot 10^{-6} \text{ L s}^{-1}$. Slightly better conditions for groundwater flow were found in the outer part, with the q value up to $6.40 \cdot 10^{-4} \text{ L s}^{-1}$, but still lower than the values calculated for the other geomorphological forms (Table 5).

Table 5.

Potential groundwater flow within individual lithological types and geomorphological forms.

	Specific groundwater runoff q (L s^{-1})		
	min.	max.	weighted average
Sediment type			
Loam	$3.18 \cdot 10^{-7}$	$4.49 \cdot 10^{-5}$	$1.61 \cdot 10^{-5}$
Sandy loam	$1.30 \cdot 10^{-5}$	$2.62 \cdot 10^{-4}$	$1.45 \cdot 10^{-4}$
Sand with debris	$3.52 \cdot 10^{-5}$	$3.78 \cdot 10^{-3}$	$8.80 \cdot 10^{-4}$
Multi-grained sand	$7.25 \cdot 10^{-4}$	$1.11 \cdot 10^{-2}$	$5.90 \cdot 10^{-3}$
Pebbly debris	$8.75 \cdot 10^{-3}$	$2.00 \cdot 10^{-1}$	$8.45 \cdot 10^{-2}$
Sandy-gravel debris	$1.75 \cdot 10^{-3}$	$5.00 \cdot 10^{-2}$	$1.82 \cdot 10^{-2}$
Loamy debris	$3.04 \cdot 10^{-4}$	$1.56 \cdot 10^{-2}$	$4.10 \cdot 10^{-3}$
Geomorphological forms			
Rocky initial soils	$1.07 \cdot 10^{-3}$	$8.75 \cdot 10^{-3}$	$1.84 \cdot 10^{-3}$
Sorted patterned ground (middle part)	$3.18 \cdot 10^{-7}$	$2.54 \cdot 10^{-4}$	$2.94 \cdot 10^{-6}$
Sorted patterned ground (outer part)	$2.62 \cdot 10^{-4}$	$3.84 \cdot 10^{-2}$	$6.40 \cdot 10^{-4}$
Pebbly alluvial sediments	$3.04 \cdot 10^{-4}$	$3.26 \cdot 10^{-2}$	$1.44 \cdot 10^{-3}$
Boulder blankets	$2.38 \cdot 10^{-2}$	$7.70 \cdot 10^{-2}$	$2.87 \cdot 10^{-2}$
Solifluction stripes	$3.34 \cdot 10^{-4}$	$3.57 \cdot 10^{-2}$	$1.86 \cdot 10^{-3}$
Talus	$7.15 \cdot 10^{-3}$	$2.00 \cdot 10^{-1}$	$3.67 \cdot 10^{-2}$
Nonsorted patterned ground	$1.62 \cdot 10^{-4}$	$5.65 \cdot 10^{-3}$	$7.60 \cdot 10^{-4}$

The total amount of the specific groundwater runoff (q_{tot}) from the Brattegg River catchment has been also calculated. The layout of the river network in the catchment is limited only to the Brattegg River, to which contribute only a few watercourses of a short length and low flow rate. Consequently, the Brattegg River is the main base for groundwater drainage. In the given scope, the efficiency of the groundwater stream flowing into the Brattegg River was estimated. The calculations were based on the average values of the hydraulic conductivity calculated for the geomorphological forms, a hydraulic gradient of 0.05 and the unit thickness of the aquifer. Data related to the variability of geomorphological forms along the Brattegg river bed were also needed as well as the results of direct observations (Fig. 5) and archived data (Fig. 1) (Jania *et al.* 1984; Migoń and Kasprzak 2013; Zwoliński *et al.* 2013; Owczarek *et al.* 2014).

The specific groundwater runoff q_{tot} from the Brattegg River catchment was calculated at 130.13 L s^{-1} . These calculations were completed for the three catchment areas: its upper part – above Myrktjørn Lake, the middle part, and the lower part – below Myrktjørn Lake (Fig. 6), showing a clear disproportion of q_{tot} in different areas. The specific groundwater runoff in the lower part is the lowest and amounts to 19.75 L s^{-1} , which is 15.2% of its total value; in the middle part it is slightly higher, *i.e.*, 25.18 L s^{-1} (19.3%) and in the upper part it is definitely the highest, *i.e.*, 85.2 L s^{-1} (65.5%). These differences are determined by the large variability in the permeability of the sediments filling the bottom of the Brattegg valley. Groundwater runoff from the parts of the catchment covered mostly by pebbly debris formations, *i.e.*, in the upper part of the catchment and the outflow from the right-hand part of catchment, accounts for 84.5% of the total groundwater runoff.

The calculated value of q_{tot} from the Brattegg River catchment in the amount of 130.13 L s^{-1} is from 15% to 47% of the average surface runoff amounting for the years 2005–2010 from 276 to 842 L s^{-1} . On the other hand, the value of q_{tot} is only 2% of the maximum flow rate of the Brattegg River measured in 2008 at $6\,595 \text{ L s}^{-1}$ (Stachnik *et al.* unpublished).

Conclusions

The sedimentary rocks of the permafrost active layer are characterized by high variability in permeability. The hydraulic conductivity, determined for 64 sediment samples, ranging from $6.37 \cdot 10^{-9}$ to $4.0 \cdot 10^{-3} \text{ m s}^{-1}$, indicate the permeability of the sediments from very low in the case of loams to very high for pebbly-gravel debris. The loose rocks in the studied catchment were formed in sedimentary environments, characterized by variable dynamics, as a result of slope processes and direct accumulation of glacial material. They were also formed in aquatic and aeolian environments. The tested sediments are relatively young and their permeability should be expected to change as a result of further

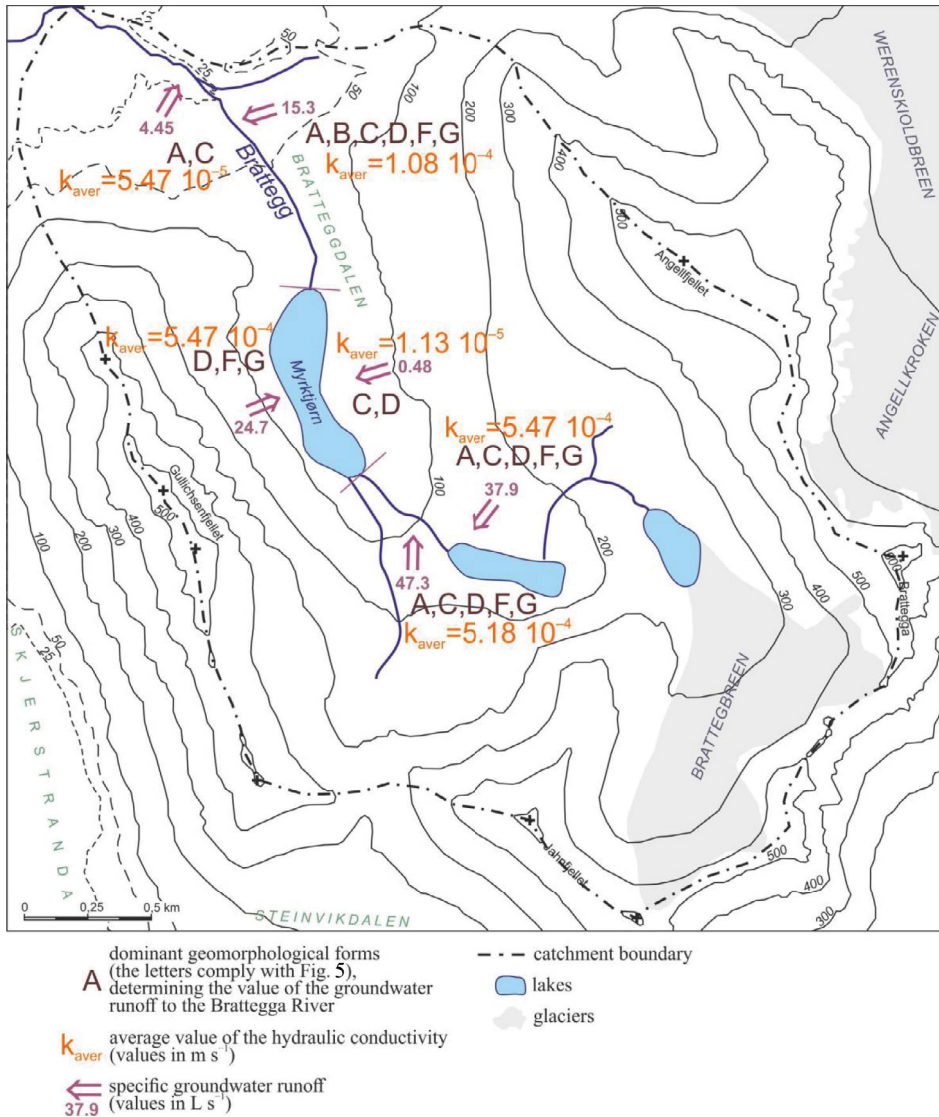


Fig. 6. Spatial distribution of the potential specific groundwater runoff in the Brattegg River catchment.

geological processes. The permeability of geomorphological forms is determined by their lithology. The highest one is estimated for boulder-pebbly covers and rock debris, and the lowest for patterned ground.

Sediment permeability is the main factor influencing the amount of the groundwater runoff, which in the major part of the studied catchment takes place most often within rock debris and boulder covers, and only to a small extent in areas with structured-polygon soils. The calculated values of the specific groundwater runoff represent the potential flow, which may be reached only

during the summer season, when the active layer is watered. In fact, for most of the year, the flow of water below the ground surface stops. In winter, the active layer of permafrost freezes. At the end of the Arctic summer, it is drained, especially in areas covered with sediments with high permeability.

Acknowledgements. — This work was supported by the funds of the Wrocław University (Project No 2213/w/ING/09). Authors would like to thank the reviewers for their comments.

References

- Bartoszewski B. and Michalczyk Z. 2013. Waters. Geographical environment in the vicinity of Calypsobyen. In: Zwoliński Z., Kostrzewski A. and Pulina M. (eds.) *Ancient and modern geoecosystems of Spitsbergen: Polish geomorphological research*. Bogucki Wydawnictwo Naukowe, Poznań: 163–169.
- Birkenmajer K. 2013. Outline of geological structure (pre-Quaternary rocks). Geographical environment in the vicinity of the Stanisław Baranowski Polar Station – Werenskioldbreen. In: Zwoliński Z., Kostrzewski A. and Pulina M. (eds.) *Ancient and modern geoecosystems of Spitsbergen: Polish geomorphological research*. Bogucki Wydawnictwo Naukowe, Poznań: 103–104.
- Burt T.P. and Williams P.J. 1976. Hydraulic conductivity in frozen soils. *Earth Surface Processes* 1: 349–360. doi: 10.1002/esp.3290010404
- Chamberlain E.J. and Gow A.J. 1979. Effect of freezing and thawing on the permeability and structure of soils. *Engineering Geology* 13: 73–92. doi: 10.1016/0013-7952(79)90022-X
- Chen J., Mei S. and Rempel A.W. 2021. Estimating permeability of partially frozen soil using floating random walks. *Water Resources Research* 57: e2021WR030598. doi: 10.1029/2021WR030598
- Czerny J., Kieres A., Manecki M. and Rajchel J. 1993. Geological map of the SW part of Wedel Jarlsberg Land Spitsbergen, 1:25 000. Institute of Geology and Mineral Deposits, University of Mining and Metallurgy, Kraków.
- Czyżewska E. 1997. *Record of flood events on the border of the Boreal and the Atlantic in the sediments of the alluvial cone in Podgordzie*. Instytut Geografii i Przestrzennego Zagospodarowania Polskiej Akademii Nauk. Wydawnictwo Continuo, Wrocław (in Polish).
- Dowgiałło J., Kleczkowski A.S., Macioszczyk T. and Rózkowski A. (eds.) 2002. *Hydrogeological dictionary*. Państwowy Instytut Geologiczny, Warszawa (in Polish).
- Duan L., Man X., Kurylyk B.L. and Cai T. 2017. Increasing winter baseflow in response to permafrost thaw and precipitation regime shifts in Northeastern China. *Water* 9: 25. doi: 10.3390/w9010025
- Eijkelkamp Agrisearch Equipment 1983. *The Double Ring Infiltrometer*. Eijkelkamp, Giesbeek (unpublished).
- Evans S.G., Ge S., Voss C.I. and Molotch N.P. 2018. The role of frozen soil in groundwater discharge predictions for warming alpine watersheds. *Water Resources Research* 54: 1599–1615. doi: 10.1002/2017WR022098
- Freeze R.A. and Cherry J.A. 1979. *Groundwater*. Prentice-Hall, Englewood Cliffs, New Jersey.
- Ge S., McKenzie J., Voss C. and Wu Q. 2011. Exchange of groundwater and surface-water mediated by permafrost response to seasonal and long term air temperature variation *Geophysical Research Letters* 38: L14402. doi: 10.1029/2011GL047911

- Hagen J.O. and Lafauconnier B. 1995. Reconstructed runoff from the high Arctic Basin Bayelva based on mass-balance measurements. *Nordic Hydrology* 26: 285–296.
- Haldorsen S. and Heim M. 1999. An Arctic groundwater system and its dependence upon climatic change: An example from Svalbard. *Permafrost and Periglacial Processes* 10: 137–149.
- Hiyama T., Asai K., Kolesnikov A.B., Gagarin L.A. and Shepelev V.V. 2013. Estimation of the residence time of permafrost groundwater in the middle of the Lena River basin, eastern Siberia *Environmental Research Letters* 8: 035040. doi: 10.1088/1748-9326/8/3/035040
- Jania J., Pulina M. and Karczewski A. (eds.) 1984. *Horsund, Spitsbergen, Geomorphology, 1:75 000*. Institute of Geophysics, Polish Academy of Sciences. Silesian University, Katowice.
- Killingveit A., Pettersson L. and Sand. 2003. Water balance investigation in Svalbard. *Polar Research* 22: 161–171. doi: 10.3402/polar.v22i2.6453
- Kim J., Jeon S.-W., Lim H.S., Lee J., Kim O.-S., Lee H. and Hong, S.G. 2020. Hydrogeological characteristics of groundwater and surface water associated with two small lake systems on King George Island, Antarctica. *Journal of Hydrology* 590: 125537. doi: 10.1016/j.jhydrol.2020.125537
- Kwaczyński J. 2003. *Meteorological yearbook Horsund 2001/2002*. Publications of the Institute of Geophysics. Polish Academy Sciences, D-60, Warszawa.
- Lamontagne-Hallé P., McKenzie J., Kurylyk B. and Zipper S. 2018. Changing groundwater discharge dynamics in permafrost regions. *Environmental Research Letters* 13: 084017. doi: 10.1088/1748-9326/aad404
- Lemieux J.-M., Fortier R., Talbot-Poulin M.-C., Molson J., Therrien R., Ouellet M., Banville D., Cochand M. and Murray R. 2016. Groundwater occurrence in cold environments: examples from Nunavik, Canada. *Hydrogeology Journal* 24: 1497–1513. doi: 10.1007/s10040-016-1411-1
- Łanczont M., 1994. Chronostratigraphy of Pleistocene and condition of their accumulation at Prałkowice near Przemyśl. *Studia Geomorphologica Carpatho-Balcanica* XXVII–XXVIII, Kraków: 16–28.
- Majchrowska E., Ignatiuk D., Jania J., Marszałek H. and Wąsik M. 2015. Seasonal and interannual variability in runoff from the Werenskioldbreen catchment, Spitsbergen. *Polish Polar Research* 36: 197–224.
- Marciniak M., Dragon K. and Chudziak Ł. 2011. The role of groundwater flow on the Ebba polar river runoff (Petuniabukta, Central Spitsbergen). *Biuletyn Państwowego Instytutu Geologicznego* 445: 371–382 (in Polish).
- Marsz A.A., Niedźwiedz T. and Styszyńska A. 2013. Modern climate changes on Spitsbergen as a basis for determining landscape metamorphosis. In: Zwoliński Z., Kostrzewski A. and Pulina M. (eds.) *Ancient and modern geocosystems of Spitsbergen: Polish geomorphological research*. Bogucki Wydawnictwo Naukowe, Poznań: 391–413.
- Marszałek H. and Górniak D. 2017. Changes in water chemistry along the newly formed High Arctic fluvial-lacustrine system of the Brattegg Valley (Wedel Jarlsberg Land, SW Spitsbergen). *Environmental Earth Sciences* 76: 449. doi: 10.1007/s12665-017-6772-9
- Marszałek H., Rysiukiewicz M., Staško S. and Wąsik M. 2013a. Waters. Geographical environment in the vicinity of the Stanisław Baranowski Polar Station – Werenskioldbreen In: Zwoliński Z., Kostrzewski A. and Pulina M. (eds.) *Ancient and modern geocosystems of Spitsbergen: Polish geomorphological research*. Bogucki Wydawnictwo Naukowe, Poznań: 125–131.
- Marszałek H., Staško S. and Wąsik M. 2013b. Estimation of subsurface runoff in the Hornsund region (SW Spitsbergen). *Biuletyn Państwowego Instytutu Geologicznego* 456: 391–395 (in Polish).
- McKenzie J.M., Voss C.I. and Siegel D.I. 2007. Groundwater flow with energy transport and water-ice phase change: Numerical simulations, benchmarks, and application to freezing in peat bogs. *Advances in Water Resources* 30: 966–983. doi: 10.1016/j.advwatres.2006.08.008

- Migała K., Nasiółkowski T. and Pereyma J. 2008. Topoclimatic conditions in the Horsund area (SW Spitsbergen) during the ablation season 2005. *Polish Polar Research* 29: 73–91.
- Migoń P. and Kasprzak M. 2013. Landforms. Geographical environment in the vicinity of the Stanisław Baranowski Polar Station -Werenskioldbreen. In: Zwoliński Z., Kostrzewski A. and Pulina M. (eds.) *Ancient and modern geocosystems of Spitsbergen: Polish geomorphological research*. Bogucki Wydawnictwo Naukowe, Poznań: 104–114.
- Modelska M. and Buczyński S. 2023. Hydrodynamics and hydrogeochemistry of the Werenskiold glacier forefield (SW Spitsbergen). *Polish Polar Research* 44: XX–YY. doi: 10.24425/ppr.2023.144540
- Myślińska E. 2001. *Laboratory soil research*. Wydawnictwo Naukowe PWN, Warszawa (in Polish).
- Owczarek P. 2010. Dendrochronological dating of geomorphic processes in the High Arctic. *Landform Analysis* 14: 45–56.
- Owczarek P., Nawrot A., Migała K., Malik I. and Korabiewski B. 2014. Flood-plain responses to contemporary climate change in small High-Arctic basins (Svalbard, Norway). *Boreas* 43: 384–402. doi: 10.1111/bor.12061
- Pazdro Z. and Kozerski B. 1990. *General hydrogeology*. Wydawnictwa Geologiczne, Warszawa (in Polish).
- Pleczyński J. 1981. *Renewal of groundwater resources*. Wydawnictwa Geologiczne, Warszawa (in Polish).
- Przybylak R. and Arażny A. 2006. Climatic condition of the north–west part of Osoat II Land (Spitsbergen) in the period between 1975 and 2000. *Polish Polar Research* 27: 139–152.
- Pulina M., Pereyma J., Kida J. and Krawczyk W. 1984. Characteristics of the polar hydrological year 1979/1980 in the Werenskiold Glacier, SW Spitsbergen. *Polish Polar Research* 5: 165–182.
- Quinton W.L., Hayashi M. and Carey S.K. 2008. Peat hydraulic conductivity in cold regions and its relation to pore size and geometry. *Hydrological Processes* 22: 2829–2837. doi: 10.1002/hyp.7027
- Racinowski R., Szczepke T. and Wach J. 2001. *Presentation and interpretation of the results of Quaternary sedimentation studies*. Wydawnictwo Uniwersytetu Śląskiego, Katowice (in Polish).
- Scheidegger M.J. 2013. *Impact of permafrost dynamics on Arctic groundwater flow systems with application to the evolution of spring and lake taliks*. Ph.D. thesis, School of Environmental Sciences, University of East Anglia.
- Sobota I. 2000. Ablation and discharge of the Waldemar Glacier, north-western Spitsbergen, in summer 1998. *Polish Polar Research* 21: 3–18.
- Sobota I., Ćmielewski M. and Nowak M. 2010. Characteristic and reasons of discharge variations of glacial river during summer time based on the Waldemar river, Svalbard. *Problemy Klimatologii Polarnej* 20: 143–159 (in Polish).
- St. Jacques J.-M. and Sauchyn D.J. 2009. Increasing winter baseflow and mean annual streamflow from possible permafrost thawing in the Northwest Territories, Canada. *Geophysical Research Letters* 36: L01401. doi: 10.1029/2008GL035822
- Walvoord M.A., Voss C.-I. and Wellman T.P. 2012. Influence of permafrost distribution on groundwater flow in the context of climate-driven permafrost thaw: example from Yukon Flats Basin, Alaska, United States. *Water Resources Research* 48: W07524. doi: 10.1029/2011WR011595
- Watanabe K. and Flury M. 2008. Capillary bundle model of hydraulic conductivity in frozen soil. *Water Resources Research* 44: 402. doi: 10.1029/2008WR007012
- Wąsik M. 2003. *Infiltration capacity of the subsurface deposits and the groundwater recharge*. Acta Universitatis Wratislaviensis 2591, Hydrogeologia. Wydawnictwo Uniwersytetu Wrocławskiego, Wrocław (in Polish).

Zwoliński Z., Giżejowski J., Karczewski A., Kasprzak M., Lankauf K. R., Migoń P., Pękala K., Repelewska-Pękalowa J., Rachlewicz G., Sobota I., Stankowski W. and Zagórski P. 2013. Geomorphological settings of Polish research areas on Spitsbergen. *Landform Analysis* 22: 125–143. doi: 10.12657/landfana.022.01

Received 8 June 2022

Accepted 12 December 2022